Available online at www.sciencedirect.com

ScienceDirect

Journal of Magnesium and Alloys 10 (2022) 3281–3287

www.elsevier.com/locate/jma

Full Length Article

Effect of crystallization on purity of volatile metallic magnesium prepared from a one-step multi-region condensation process under vacuum condition

Bin Yang[a,b,c], Dong Liang[a,b,c], Neng Xiong[d], Yang Tian[a,b,c,*], Baoqiang Xu[a,b,c], Yongnian Dai[a,b,c]

[a] *The State Key Laboratory of Complex Non-ferrous Metal Resources Clean Utilization, Kunming University of Science and Technology, Kunming 650093, China*

[b] *National Engineering Laboratory for Vacuum Metallurgy, Kunming University of Science and Technology, Kunming 650093, China*

[c] *Faculty of Metallurgical and Energy Engineering, Kunming University of Science and Technology, Kunming 650093, China*

[d] *IME Institute of Process Metallurgy and Metal Recycling, RWTH Aachen University, Aachen 52056, Germany*

Received 20 April 2021; received in revised form 6 July 2021; accepted 3 August 2021
Available online 14 September 2021

Abstract

We hereby report a green and simple volatilization-condensation process to prepare high-purity magnesium in different crystal forms under vacuum condition. This method can be also used for the analysis of other metals, which can be separated by the same concept. In addition, Mg condensation is a very fast process, and the corresponding easy growth of the Mg crystals is promoted when the concentration of magnesium vapor is raised. From the view of crystallization, ultrafast crystal growth of high-purity magnesium is a barrier-free and orderly process. Interestingly, different condensed forms of Mg obtained via this ultrafast volatilization-condensation process are showing different purities. The distinct morphological formation of Mg in different condensed form is probably attributed to the differences of surface energy change of Mg during the condensation process.

Keywords: Mg; Purity; Vacuum; Condensation; Crystallization.

1. Introduction

As a basic element, magnesium and Mg-based materials have properties such as lightweight, high specific strength, strong electromagnetic shielding ability and so on. Thanks to these advantages, Mg is widely used in high-tech fields like electronics, aerospace, and precision instruments [1–5]. Generally, achieving precise purity control is one of the most important steps to design materials, because of the inferiority of impurities. For example, Mg alloys show higher corrosion rates than that of high-purity (HP) Mg (above 99.98%, wt.%), which is caused by a higher impurity content [6–8]. In addition, it has been shown that the purification treatment can be employed to slow down the biodegradation of the magnesium alloys [9]. Hence, the control of purity is very important for magnesium-based materials.

At present, the purification of magnesium is mainly classified into chemical methods and physical methods, such as melt purification [7,10,11], additive refining [12,13], electrolytic refining [14], and vacuum distillation [8,15–19]. Among those methods, the refined magnesium obtained by vacuum distillation has the lowest impurity content. The effective additive refining purification cannot be used alone, and the other methods are all costly and complex processes. On the other hand, vacuum technology has been successfully applied to the researches of separation, purification, and recycling of heavy metals [20,21], precious metals [22–24], scattered nonmetals [25] and rare metals [26]. But up to now, there are nearly no studies reported on volatile metals which with high saturated vapor pressure (such as Mg, Zn). So,

* Corresponding author at: Faculty of Metallurgical and Energy Engineering, Kunming University of Science and Technology, Kunming 650093, China. E-mail address: emontian@hotmail.com (Y Tian).

https://doi.org/10.1016/j.jma.2021.08.008

vacuum distillation is expected to be a very promising and environment-friendly purification technology for volatile metals because of its high efficiency in relation to not only the removal of impurities but also the simple and effective of the process. However, despite some observations [8,19,27], experimental parameters and influencing factors for obtaining high-purity or even ultra-pure magnesium have not been clearly clarified, which significantly limits the application of this technology.

In this work, a horizontal tubular furnace, which is different from the traditional equipment, is used in the experiments. The tubular cavity with sufficient length has a function of horizontal axial temperature distribution under vacuum condition. A special design of the volatilization step allows the raw magnesium sample to quickly evaporate into a form of magnesium vapor. The effect of crystal formation on the purity of the condensate Mg prepared with this horizontal tubular furnace is studied at different evaporation temperatures. This is considered as a key factor for efficient production of high-purity Mg and maybe also other metals. This would also probably form a theoretical basis and provide fundamental data for Mg purification mechanisms.

2. Methods

2.1. Theoretical considerations of vacuum distillation

Impurities in raw materials can be removed during the volatilization process due to different saturated vapor pressure of each element. The relationship between the saturated vapor pressure and the temperature of pure substances can be expressed as following [28]:

$$\lg p* = AT^{-1} + B\lg T + CT + D \quad (1)$$

where p^* is the saturated vapor pressure of a certain pure substance, and *A, B, C* and *D* are the evaporation constants of each element in the alloy. The order of volatilization of impurity elements in the distillation process is dependent on their saturated vapor pressures, i.e., the substance with a higher vapor pressure tends to be evaporated prior to those with lower vapor pressures in the volatilization process.

2.2. Horizontal tubular furnace for one-step multi-region condensation process

It is found in the previous researches that, the traditional vertical vacuum furnace is the most well-known and widely-used vacuum equipment for non-volatile metals [8,20–26]. For this type of furnace, raw material located in the bottom heating zone of the furnace is firstly converted from solid to liquid by elevating temperature. Afterward, the metals in the molten phase are volatilized in order from the high to the low saturated vapor pressure. Subsequently, the gaseous metals rise and finally transfer into the solid-state after reaching the inner surface of the top furnace cover with a lower temperature. However, for the volatilization of volatile metals, it has to be noted that, e.g., the solid magnesium does not go through a liquid phase at system pressures below 333 Pa [27], which leads to a faster volatilization and condensation process of magnesium. Despite this advantage of the high efficiency of the process, it is very challenging to obtain accurate experimental parameters such as the volatilization time and the condensation temperature by using the traditional type of furnaces. More importantly after contacting the colder surface, the magnesium vapor would directly sublimate into solid particles on one metal plate with uneven size. This is a challenge for the collection of the condensed products, because there is a potential risk of explosion for the magnesium powders of smaller size.

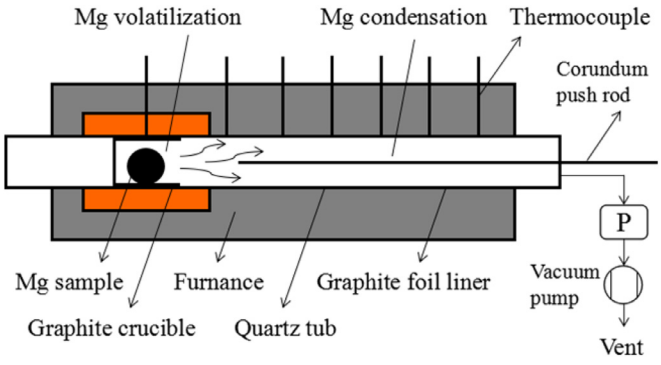

Fig. 1. Schematic of Mg volatilization-condensation system with distinct regions for (1) Mg volatilization and (2) Mg condensation.

On the other hand, a multi-stage condenser has been designed and realized for a better separation of condensation products [23]. The multi-layer concave graphite platform can prevent the metals in liquid phase from slipping. Each platform has a small hole that allows gaseous products to pass through. However, the design of such equipment is complicated and expensive. In addition, due to fluctuations in the thermal field of this equipment, the material obtained on each platform is not completely uniform. Therefore, an additional experimental procedure of heating first and then sampling has been complemented. The volatilization and condensation can proceed synchronously in one chamber but in different temperature regions, as shown in Fig. 1. Based on the previous investigation of the volatilization and condensation behaviors of magnesium [27], it is deemed that the deposits with a heavier mass, a denser aggregation degree and a larger grain size can be attained in the higher condensation temperature area (close to the heating source). During the condensation process, it can be hypothesized that each temperature gradient corresponding to the positions with different grain size is stable. The condensed magnesium with different grain sizes can be obtained conveniently in one process. With a clear axial distribution, different grains can be directly used as specimens for material characterizations.

2.3. Experimental procedure of Mg volatilization and condensation

Magnesium ingot (99.98%, Henan Yuhang Materials, China) was selected as raw material (Fig. 2a), the typically

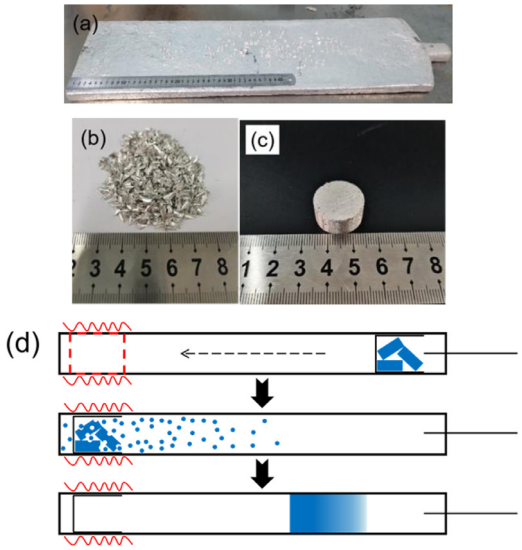

Fig. 2. (a) Picture of magnesium ingot; (b) Picture of magnesium strips; (c) Picture of magnesium block; (d) Schematic of the sampling step, volatilization and condensation process.

Table 1.
Types and content of impurities in magnesium ingots (ppm).

Element	Al	Mn	Fe	Ni	Cu	Zn	Si	Ca
Content	4.8	20.0	11.5	1.0	1.6	24.0	37.0	25.0

impurities contents detected by ICP-MS in magnesium ingot were shown in Table 1. It was firstly drilled to prepare magnesium strips, and then these strips were washed twice with ethanol. Afterwards, they are dried with a filter paper and accordingly show a bright surface (Fig. 2b). The prepared samples were transported with zip-lock plastic bags in the whole process. The preparation of magnesium block samples should be carried out as fast as possible to avoid excessive and unnecessary surface oxidation. In a later step, the magnesium blocks (Fig. 2c) were pressed using a mold. 20 g Mg blocks were placed in a cylindrical graphite crucible close to the condensing zone. A graphite paper was used to fully cover the inner wall of the quartz tube. High-purity crystallized Mg particles and flakes condensed on the graphite paper were collected and then characterized with different kinds of material analytical tools. When the heating temperature was stabilized in the range of 700–850 °C under a system pressure of 10 Pa, graphite crucible with Mg blocks were pushed together to the heating zone by a corundum pusher. Those samples were completely evaporated within 30 min (Fig. 2d).

The yielding Mg condensation products were collected from the surface of the graphite paper in the area of lower temperature. The raw material was rapidly evaporated in the zone of volatilization, and the correspondingly generated magnesium vapor condensed into a solid phase when it encountered a low-temperature interface. Since the high-temperature gaseous magnesium atoms of random motion were more energetic than those in the solid-state, they condensed on both the left and the right sides of the heating zone. However,

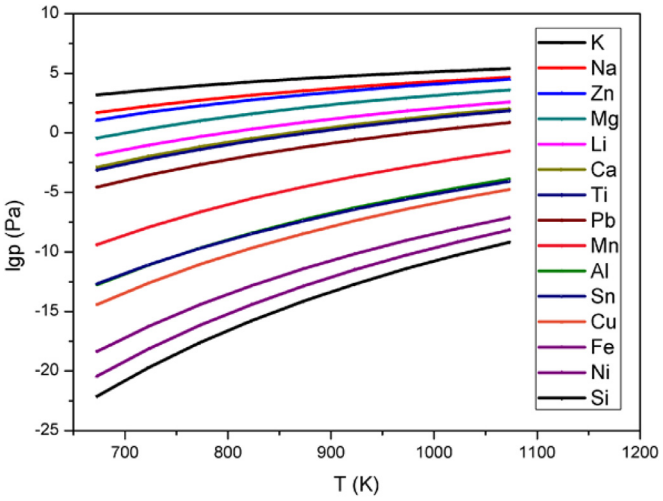

Fig. 3. The relationship between saturated vapor pressure of different metals and temperature.

the temperature at the location where the condensates were formed on the left side was difficult to measure. As a consequence, only the products obtained in the right condensing zone were collected for further analysis and characterization.

2.4. Material characterization

The morphological structures of the Mg blocks and the condensation products were characterized by scanning electron microscopy (SEM, TM3030 Plus, Hitachi). The crystal structure of the condensed Mg at different condensation temperatures was studied by X-ray diffraction (XRD) using a PANalytical EMPYREAN with a Cu Kα of 1 °/min. The purity of the condensation samples was characterized by inductively coupled mass spectrometry (ICP-MS, 7700x ICP-MS, Agilent).

3. Results and discussion

Fig. 3 shows the difference of saturated vapor pressures of impurity elements and magnesium, according to the formula (1) introduced in Section 2.1, it can be seen that the saturated vapor pressure of every single substance in the magnesium-based raw material increases with rising of the temperature. At the same temperature, the saturated vapor pressures of K, Na and Zn are higher than that of Mg. This means they would be evaporated before the solid Mg turn into a gas phase in the distillation process. On the contrary, the other metals, like Ca, Ti, Pb, Mn, Al, Sn, Cu, Fe, Ni, and Si, generally share a non-volatile property and remain in the liquid phase in the distillation process. Theoretically, the advantage of vacuum purification technology is that the target metal can be separated by its specific saturated vapor pressure different from those of the interfering metals. The purpose of this work is to study the effect of the crystallization state on the purity of the condensed Mg. Therefore, the usage of the horizontal tubular furnace offers a convenient and effective way to obtain dif-

ferent crystallization Mg-samples in the one-step multi-region condensation process under vacuum condition, because the temperature gradient formed in the quartz tube (Fig. 1) enable the formation of the condensed Mg with different morphological and crystal structures.

Fig. 4(a–d) shows the products of magnesium vapor condensed on the graphite paper. The initial section (the left part) of graphite paper in the picture here has been cut off. This is because there were no products on the graphite paper in this section (Fig. 2d). Another reason is that considering the length of the graphite paper, it is trying to provide enough size for the SEM images. It can be seen that the condensed Mg in silver-white color locates in different condensation temperature regions and show different physical forms. The experimental results at four different volatilization temperatures (700, 750, 800, 850 °C) show that the condensation temperatures of magnesium vapor are consistent, all of which are in a range of 330–460 °C. The yielding Mg-products close to the source of the volatilization are in the form of an integral piece with the uneven surface formed by large size particles, while smaller-sized particles are relatively far from the volatilization source. This phenomenon is consistent with the results of Han's research under Ar air flow, that is, the condensation products of magnesium include droplet magnesium, transitional condensed magnesium and powder magnesium [29,30]. The metallic magnesium crystal with a hexagonal structure can be easily and clearly seen from the SEM shown in Fig. 4a. Accordingly, it is shown that the typical grain size of the magnesium flake is 300–500 μm, and the typical grain size of those smaller particles is around 10 μm. As expected, the crystal accumulation is denser in the area with the higher condensation temperature but scattered in the area with the lower condensation temperature. In addition, the maximum temperature in the condensation area is more than 100 °C lower than the melting point of magnesium. Combining the laws of the magnesium vapor volatilization and the condensation, it brings light to the interesting fact that the condensation of magnesium vapor is an ultra-fast cooling process under these experimental conditions.

There are two elements, Mg and O found in corresponding energy dispersive spectrometer (EDS) analysis, which has not been shown here. This indicates, the condensed Mg may be slightly oxidized in the process. But, the element contents by this semi-quantitative analysis may not be reliable without proper error estimation. Therefore, a better quantitative identification is conducted with the ICP analysis. Moreover, X-ray diffraction (XRD) patterns (Fig. 4e and f) also confirm the crystalline characteristics of the condensation Mg-products after volatilization-condensation processes. As shown in Fig. 4, the prominent interfaces of the hexagonal close-packed (hcp) crystal exhibit different growth kinetics, which means the process is dominated by lateral growth.

The ICP-MS analysis is used to investigate the level of impurities in Mg condensation products with different crystal forms and accordingly evaluate the effect of purification. The condensed magnesium in the integrated flake form is postulated to be better crystallized and contain a lower content level of impurities. This assumption was confirmed by the ICP-MS analysis. The contents of the impurities in the condensed Mg products with the flake form in the higher condensation temperature region and the products with the granular form in the lower condensation temperature region are shown in Table 2. From this analysis, it can be inferred that the purity of the condensed Mg-products is correlated with its macroscopic structural form and microscopic grain size. That is to say, the lower impurity content is probably a consequence of (i) a larger grain size formed in the condensation process, and (ii) correspondingly their accumulation to the integral flake Mg. And this result is consistent with the theory analysis referred above and the Han's research, the condensation products obtained in higher temperature zone has higher purity [31]. These results reveal that the purity of the condensed Mg is highly affected by the degree of crystallization in the condensation process. It can be seen that, the integrated magnesium flakes with very high purity can be prepared via this rapid volatilization-condensation process. Moreover, the Mg particles in the lower temperature area can be further purified by an additional melting/refining process, which may clearly reduce the potential risk of explosion of those very fine magnesium powders.

Table 2.
The contents of impurities in the higher condensation temperature region and lower temperature region (ppm).

Element	Al	Mn	Fe	Ni	Cu	Zn	Si	Ca
1#	<DL	1.24	<DL	<DL	<DL	13.61	<DL	21.61
2#	9.81	43.46	33.93	0.39	<DL	243.13	<DL	39.42

(The magnesium product in higher condensation temperature was marked as 1#, the magnesium product in lower condensation temperature was marked as 2#, "<DL" means the value is lower than the detection limit).

The process of the internal crystal growth of the magnesium after vacuum distillation is rearranged to in relation to the raw material. After the metal vapor of Mg has reached the saturated temperature, the process of cooling and condensing would start to take place and form a condensed phase. The condensation process may proceed in two different ways. Namely, they are (i) the gaseous Mg vapor forms the small particles (nuclei) of the condensed state in the gas phase, and they later grow up gradually. This way is also known as the spontaneous nucleation. (ii) As shown by the clear condensate edge in Fig. 4, the high temperature magnesium vapor condenses rapidly on the low temperature graphite paper, i.e., the condensation process occurs on the medium. The surface structure and the Gibbs-free energy of a crystal vary with the crystallographic orientation. A general approach for controlling the shape is to grow the crystal in the presence of species that bind with different adsorption energies to the different crystalline facets [32].

The volatilization disrupts the order of the interfacial inherent structures of magnesium blocks, and consequently the re-organization has been activated before ordering in the crystallization. If concretely, we confine our attention to the crys-

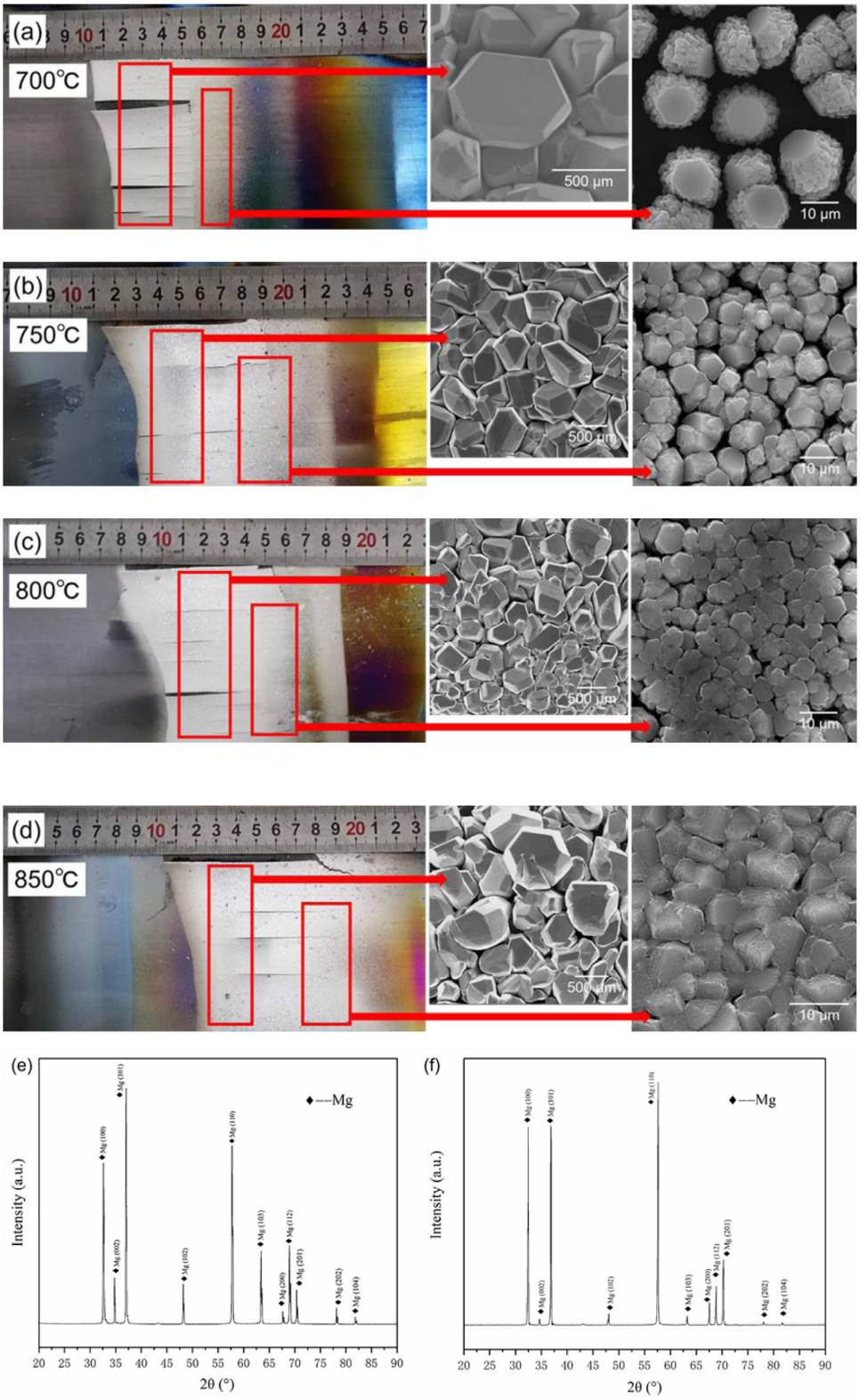

Fig. 4. (a–d) Pictures of the condensed magnesium from different heating temperature (700, 750, 800, 850 °C) attached on graphite paper, and SEM images of the products in higher and lower condensation temperature regions, respectively. (e, f) XRD patterns of condensed flake and particles, respectively.

tals, it is found that the condensed flakes from the condensation process have a close-packed surface. The surface atoms of one height are at the same distance from a plane parallel to it, and the surface presents a stepped appearance. The condensation on a close-packed surface can only take place by surface nucleation. This means, the small "islands" of the Mg-atoms are accumulated on the surface and gradually grow to a new layer. The Mg-vapor in this process shows a high supersaturation. In addition, the growth essentially depends on the existence of "kinks" on the surface [33]. The easy growth of the Mg-layer in the condensation process is promoted when the concentration of the magnesium vapor is raised. The average evaporation rate in the experiments may even reach a maximum, 3.947×10^{-4} g/(cm^2•s) in 10 min [27]. This indicates that condensation is a very fast process, even though it is not able to be quantitatively analyzed at the moment. There were already pre-condensed magnesium particles available as suitable deposition points (kinks) before the magnesium vapor with high concentration was transported to the condensation zone.

Based on the determination of the rapid condensation, there is no supercooled Mg liquid order sufficiently to interfere with the propagation of a crystal interface at subcooling in 190–300 K. It means that the propagation of the crystal interface is not disturbed and the growth of the condensate is well ordered. Even though the ultrafast crystal growth in the high-purity magnesium is a barrierless ordering process, the fundamental reason is different from the process of liquid solidification, which is achieved by imposing a crystalline inherent structure onto the adjacent liquid due to the capacity of the crystal interface [34]. The crystal interface in the pure magnesium seems to be an important factor to establish the ordered interfacial inherent structures. The reduction in the surface energy is the primary driving force for the simple particle growth, while the morphological evolution is driven by the further reduction of the surface energy due to the minimization of the area of the high energetic crystal faces [35]. In the process of the gaseous Mg atoms transferred to the condensation zone for crystallization, the change of the surface energy of the impurities and the target metal (Mg) promotes the condensation products to develop into different forms, respectively. Quantitative studies, such as modeling and dynamics simulation, need to be carried out in the future to confirm the process of ultrafast crystallization.

4. Conclusion

In summary, we have demonstrated that the high-purity magnesium with different crystal forms can be obtained from a one-step approach without a time-consuming and polluting procedure. This research concept can be also applied to other kinds of volatile metals. The ultrafast solidification and the growth of high-purity magnesium crystals are both a barrier-free and orderly processes. Two different macroscopic structural forms, namely the flake form and the granular form, particles are found to be formed in the condensation process depending on the temperature, respectively. More significantly, different condensed forms obtained through this ultrafast volatilization-condensation process are noted to show different purity levels. Furthermore, different surface energy change of Mg during the condensation process drives the morphological evolution, which can be further validated by modeling and dynamics simulation. Our research offers a new possibility to analyze the effect of crystallization on the purity of the condensed Mg during the condensation process. This may provide fundamental data for the mechanisms of the Mg purification and hopefully open up opportunities for the effective production of high purity metals.

Declaration of Competing Interest

The authors declare that they have no known competing financial interests or personal relationships that could have appeared to influence the work reported in this paper.

Acknowledgements

This research was supported by the Basic Research Project of Yunnan Province [No. 2019FB080]; and by the Scientist Studio of Yunnan Province.

References

[1] B.L. Mordike, T. Ebert, Mater. Sci. Eng. A. 302 (1) (2001) 37–45, doi:10.1016/S0921-5093(00)01351-4.
[2] I.J. Polmear, Mater. Sci. Technol. 10 (1994) 1–16, doi:10.1179/mst.1994.10.1.1.
[3] Z.R. Zeng, N. Stanford, C.H.J. Davies, J.F. Nie, N. Birbilis, Int. Mater. Rev. 64 (2019) 27–62, doi:10.1080/09506608.2017.1421439.
[4] A.A. Luo, Int. Mater. Rev. 49 (2004) 37–45, doi:10.1179/095066004225010497.
[5] N. Li, Y.F. Zheng, J. Mater. Sci. Technol. 29 (2013) 489–502, doi:10.1016/j.jmst.2013.02.005.
[6] N. Ishida, Z. Abidin, A.D. Atrens, D. Martin, A. Atrens, Corros. Sci. 533 (2011) 542–3556, doi:10.1016/j.corsci.2011.06.030.
[7] A. Prasad, P.J. Uggowitzer, Z.M. Shi, A. Atrens, Adv. Eng. Mater. 14 (7) (2012) 477–490 http://10.1002/adem.201200054, doi:10.1002/adem.201200054.
[8] Y.C. Wang, Y. Tian, T. Qu, B. Yang, Y.N. Dai, Y.P. Sun, Mater. Sci. Forum 788 (2014) 52–57, doi:10.4028/www.scientific.net/MSF.788.52.
[9] G.L. Song, Corros. Sci. 49 (2007) 1696–1701, doi:10.1016/j.corsci.2007.01.001.
[10] F.S. Pan, X.H. Chen, T. Yan, T.T. Liu, J.J. Mao, W. Luo, Q. Wang, J. Peng, A.T. Tang, B. Jiang, J. Magnes. Alloy 4 (2016) 8–14 http://10.1016/j.jma.2016.02.003, doi:10.1016/j.jma.2016.02.003.
[11] G.H. Wu, J.C. Dai, M. Sun, W.J. Ding, Trans. Nonferr. Metal Soc. 20 (2010) 2037–2045 http://10.1016/S1003-6326(09)60414-3, doi:10.1016/S1003-6326(09)60414-3.
[12] L.F. Zhang, T. Dupont, Mater. Sci. Forum 546-549 (2007) 25–36, doi:10.4028/www.scientific.net/MSF.546-549.25.
[13] X.S. Xue, Z.L. Zhao, Light Metals (CN) 10 (1994) 32–35 http://www.cqvip.com/QK/91164X/199410/1448797.html.
[14] J. Park, Y. Jung, P. Kusumah, B. Dilasari, H. Ku, H. Kim, K. Kwon, C.K. Lee, Met. Mater. Int. 22 (2016) 907–914 http://10.1007/s12540-016-5605-9, doi:10.1007/s12540-016-5605-9.
[15] G. Revel, J.L. Pastol, J.C. Rouchaud, R. Fromageau, Metall. Mater. Trans. B 9 (1978) 665–672 http://10.1007/BF03257216, doi:10.1007/BF03257216.
[16] M. Inoue, M. Iwai, K. Matsuzawa, Y. Kamado, S. Kojima, Mater. Sci. Forum 419-422 (2003) 691–696 http://10.4028/www.scientific.net/MSF.419-422.691, doi:10.4028/www.scientific.net/MSF.419-422.691.

[17] M. Inoue, T. Doi, T. Aida, K. Matsuki, S. Kamado, Y. Kojima, Mater. Sci. Forum 475-479 (2005) 513–516 http://10.4028/www.scientific.net/MSF.475-479.513, doi:10.4028/www.scientific.net/MSF.475-479.513.

[18 R.K.F. Lam, D.R. Marx, Ultra High Purity Magnesium Vacuum Distillation Purification method[P], U S, 1996.

[19] S.R. Mohamed, S. Friedrich, B. Friedrich, Metals 9 (2019) 85 (Basel) http://10.3390/met9010085 , doi:10.3390/met9010085.

[20] T.T. Liu, K.Q. Qiu, J. Hazard. Mater. 347 (2018) 334–340, doi:10.3390/met9010085.

[21] B. Yang, G.Z. Zha, W. Hartley, X.F. Kong, D.C. Liu, B.Q. Xu, W.L. Jiang, X.Y. Guo, J. Clean. Prod. 219 (2019) 110–116, doi:10.1016/j.jclepro.2019.02.011.

[22] G.Z. Zha, C.F. Yang, Y.K. Wang, X.Y. Guo, W.L. Jiang, B. Yang, Sep. Purif. Technol. 209 (2019) 863–869 https://10.1016/j.seppur.2018.09.038, doi:10.1016/j.seppur.2018.09.038.

[23] G.Z. Zha, B. Yang, C.F. Yang, X.Y. Guo, W.L. Jiang, JOM 71 (2019) 2413–2419 https://10.1007/s11837-019-03479-8, doi:10.1007/s11837-019-03479-8.

[24] B. Yang, D.X. Huang, D.C. Liu, G.Z. Zha, W.L. Jiang, X.F. Kong, Sep. Purif. Technol. 236 (2020) 116309 https://10.1016/j.seppur.2019.116309, doi:10.1016/j.seppur.2019.116309.

[25] G.Z. Zha, M.Q.Chne Y.K.Wang, D.X. Huang, W.L. Jiang, B.Q. Xu, B. Yang, J. Mater. Res. Technol. 9 (2020) 2926–2933 https://10.1016/j.jmrt.2020.01.043, doi:10.1016/j.jmrt.2020.01.043.

[26] X.F. Zhang, D.X. Huang, W.L. Jiang, G. Zha, J. Deng, P. Deng, X.F. Kong, D.C. Liu, Sep. Purif. Technol. 230 (2020) 15864, doi:10.1016/j.seppur.2019.115864.

[27] N. Xiong, Y. Tian, B. Yang, B.Q. Xu, D.C. Liu, Y.N. Dai, Vacuum 156 (2018) 463–468, doi:10.1016/j.vacuum.2018.08.014.

[28] Y.N. Dai, B. Yang, Non-ferrous Metal Vacuum Metallurgy, 2nd ed., Metallurgical Industry Press, Beijing, 2009.

[29] J.B. Han, T.A. Zhang, D.X. Fu, J.H. Guo, Z.H. Ji, Z.H. Dou, Metall. Mater. Trans. B 51b (2020) 1–10, doi:10.1007/s11663-020-01993-8.

[30] J.B. Han, D.X. Fu, J.H. Guo, Z.H. Ji, T.A. Zhang, Vacuum (2021) 189, doi:10.1016/j.vacuum.2021.110227.

[31] J.B. Han, D.X. Fu, J.H. Guo, Z.H. Ji, Z.H. Dou, T.A. Zhang, Metals 10 (2020) 1–16 (Basel), doi:10.3390/met10111441.

[32] A. Selloni, Nat. Mater. 7 (2008) 613–615 https://10.1038/nmat2241, doi:10.1038/nmat2241.

[33] W.K. Burton, N. Cabrera, Discuss. Faraday Soc. (1949) 33–39 https://10.1039/DF9490500033, doi:10.1039/DF9490500033.

[34] G. Sun, J. Xu, P. Harrowell, Nat. Mater. 17 (2018) 881–886 https://10.1038/s41563-018-0174-6, doi:10.1038/s41563-018-0174-6.

[35] R.L. Penn, J.F. Banfield, Geochim. Cosmochim. Acta 63 (10) (1999) 1549–1557 https://10.1016/S0016-7037(99)00037-X, doi:10.1016/S0016-7037(99)00037-X.